Incident detection and isolation in drilling using analytical redundancy relations

Willersrud, Anders; Blanke, Mogens; Imsland, Lars

Published in:
Control Engineering Practice

Link to article, DOI:
10.1016/j.conengprac.2015.03.010

Publication date:
2015

Document Version
Peer reviewed version

Incident detection and isolation in drilling using analytical redundancy relations

Anders Willersrud[a,*], Mogens Blanke[b,c], Lars Imsland[a]

[a] *Department of Engineering Cybernetics, Norwegian University of Science and Technology, N-7491 Trondheim, Norway,* {anders.willersrud,lars.imsland}@itk.ntnu.no.
[b] *Automation and Control Group, Department of Electrical Engineering, Technical University of Denmark, DK 2800 Kgs. Lyngby, Denmark,* mb@elektro.dtu.dk.
[c] *AMOS Centre of Excellence, Department of Engineering Cybernetics, Norwegian University of Science and Technology, N-7491 Trondheim, Norway.*

Abstract

Early diagnosis of incidents that could delay or endanger a drilling operation for oil or gas is essential to limit field development costs. Warnings about downhole incidents should come early enough to allow intervention before it develops to a threat, but this is difficult, since false alarms must be avoided. This paper employs model-based diagnosis using analytical redundancy relations to obtain residuals which are affected differently by the different incidents. Residuals are found to be non-Gaussian - they follow a multivariate t-distribution - hence, a dedicated generalized likelihood ratio test is applied for change detection. Data from a 1400 meter horizontal flow loop test facility is used to assess the diagnosis method. Diagnosis properties of the method are investigated assuming either with available downhole pressure sensors through wired drill pipe or with only topside measurements available. In the latter case, isolation capability is shown to be reduced to group-wise isolation, but the method would still detect all serious events with the prescribed false alarm probability.

Keywords: Managed pressure drilling, fault detection and isolation, analytical redundancy relations, multivariate change detection, generalized likelihood ratio test

*Corresponding author.

1. Introduction

Drilling for oil and gas is a high-cost operation with risk of delays, and possibly safety and environmental impacts, if an abnormal incident is occurring. A drillstring is rotated with a drill bit at the bottom, crushing the formation. A circulated drilling fluid then transports the formation cuttings back to the surface through the annulus surrounding the drillstring, see Fig. 1. Pressure in the well is controlled by the hydrostatic and friction pressure drop of the drilling fluid, as well as a possible topside back-pressure. For some wells, the pressure window of operation between the pressure of the formation fluid and the formation fracture pressure is quite narrow. Incidents happening can make it difficult to maintain this operational window, and may lead to costly delays in progress.

Monitoring of the drilling process has traditionally been done manually by drilling operators. With new sensor technology, giving an increased number of measurements available, manual monitoring may be overwhelming and tiresome for operators, whose main task is to drill deeper into the formation, maintaining operating requirements. An automatic diagnosis algorithm can be used to interpret the signals and alarming the operators at an earlier stage if something abnormal is about to develop. Abnormal downhole incidents include *influx* of fluids from the formation, or *lost circulation* of drilling fluid to the formation, *plugging of the drill bit*, *pack-off* of formation solids around the drillstring, and leakage from the drillstring to the annulus caused by wear and tear, called *drillstring washout*. Sensors may stop working, or have a slowly varying bias drift giving incorrect readings, and actuators may stop or be partially defective. If the drilling technology *managed pressure drilling* (MPD) is applied, the installed choke may be *plugged*.

Detection of influxes was studied in [1, 2]. Detection of other incidents was studied in [3] using a high-fidelity model, and a knowledge-based method was used in [4]. Lost circulation, formation fluid influx, and drillstring washout have many similarities to the problem of leak diagnosis in open water channels, see, e.g., [5].

Model-based fault diagnosis methods can often be divided into methods detecting changes in estimated parameters or states, or using residuals which are zero in the fault-free case and non-zero during a fault [6]. Diagnosis based on parameter estimation in drilling was the topic in [7, 8], while this paper presents a *fault detection and isolation* (FDI) method based on residuals generated using *analytical redundancy relations* (ARR), see, e.g., [9, 10, 11].

Model-based fault diagnosis of sensors in aircrafts using an extended Kalman filter was studied in [12], and in [13] diagnosis of actuator faults was done using analytical redundancy relations and a cumulative sum (CUSUM) method, while [14] applied ARR for an electrical distribution system.

Analytical redundancy relations offer an alternative to parameter and/or state estimation, where a structured method is used to generate residuals based on the model equations. This avoids the need for a stable adaptive observer. In addition, the ARR residual generation framework offers possibilities to detect and isolate actuator and measurements faults such as bias drift, differentiating them from process faults in a systematic manner.

Measurement noise will affect the residuals, and with small changes in the residuals due to faults, a statistical change detection algorithm is necessary. To increase detection and isolation capabilities it was demonstrated in [7] that a multivariate change detection algorithm using a *generalized likelihood ratio test* (GLRT) was superior to univariate change detection of estimated parameters. Statistical evaluation of residual signals for fault detection and isolation was studied in [15, 16, 17, 18], while the use of directional residuals was studied in [19, 20, 21].

In this paper actuator faults, sensors faults, and downhole drilling incidents are detected and isolated using a model-based fault diagnosis method. The different incidents are illustrated in Fig. 1, highlighted in red. Residuals are generated using analytical redundancy relations, which due to use of sensor measurements are affected by noise. Therefore, statistical change detection is applied using GLRT, detecting changes in the vector residual. This method will increase detectability of small changes to the process due to an incident, decreasing the false alarm rate. The different incidents will affect the residuals differently, making isolation possible by determining the residual change direction.

The method is tested on a series of data sets from a medium-scale flow loop test carried out in Stavanger, Norway. The flow loop is a horizontal loop of 1400 meters, using water as drilling fluid. The paper describes two scenarios of fault detection and isolation possibilities. In the first scenario, downhole pressure measurements are available assuming the use of *wired drill pipe* technology, see, e.g., [22, 23]. The second scenario describes what can and cannot be detected and isolated with only topside sensors available, a case still most common in the industry.

The paper is organized into ten sections. After the introduction, details about the flow-loop test setup is described in Sec. 2. Model-based fault

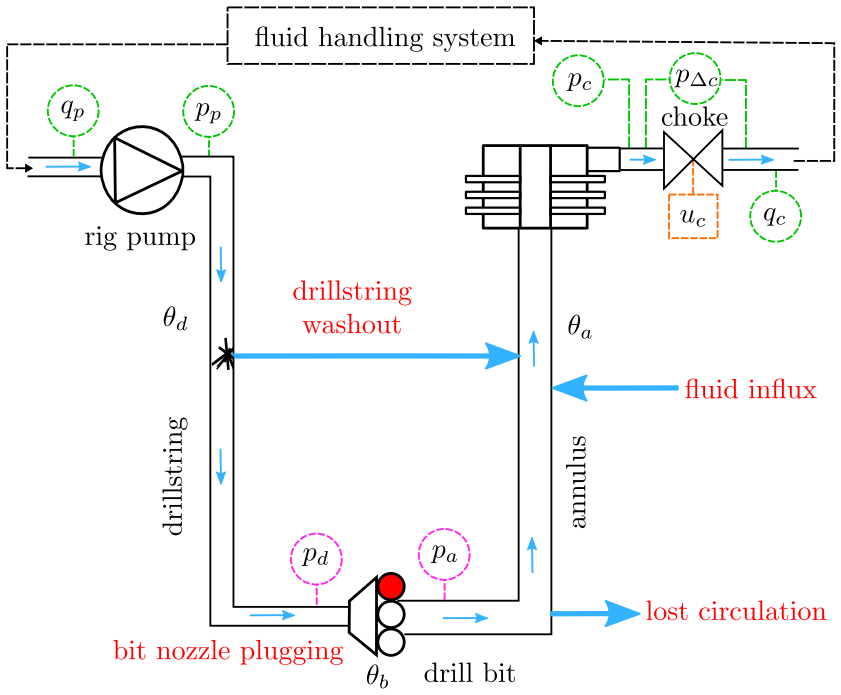

Figure 1: Managed pressure drilling process with possible downhole incidents shown in red, including lost circulation, drillstring washout, formation fluid influx, and bit nozzle plugging. Topside sensors shown in green, downhole sensors in magenta, and the actuator in orange.

diagnosis is briefly introduced in Sec. 3, and the system model is presented in Sec. 4. Analytical redundancy relations are derived in Sec. 5, and methods for change detection and incident isolation are suggested in Sec. 6. Results of incident detection and isolation using downhole sensors are shown in Sec. 7, and without downhole sensors in Sec. 8. A discussion and a conclusion finalize the paper.

2. Flow loop for testing of incidents in drilling

Data from a medium-scale horizontal flow loop is used to test fault diagnosis of downhole incidents, actuator fault, and sensor bias drift. The flow loop shown in Fig. 2 is a 1400 meter test rig located in Stavanger, Norway, circulating water in circular pipes with typical drilling diameters. During the tests the flow loop was rigged for managed pressure drilling (MPD). This

is a drilling method where the annulus is sealed off with a choke as illustrated in Fig. 1. Doing so, the downhole pressure is controlled by the choke back-pressure, which is affected by hydrostatic pressure due to density, and friction due to fluid flow. The model used in the diagnosis is thus adapted to MPD, which could be applied to conventional drilling by omitting the choke. The test setup was rigged to test the incidents bit nozzle plugging, drillstring washout, lost circulation, gas influx and choke plugging. Pack-off was not tested. No tests were done for bias drift, and this is therefore tested by artificially adding a noise-free signal to specific measurements, ramping up from zero to a constant bias.

There are some obvious differences between the test setup and real drilling. One discrepancy is the lack of difference in height between the bit at the bottom of the well and the choke at the top. This will result in different hydrostatic pressure, where during an influx the height difference will affect the now multi-phase flow. However, for normal drilling conditions, this issue only adds a constant hydrostatic pressure. Other characteristics that differ are the lack of transported solids due to drilling ahead, as well as lack of annular effects since circular pipes are used in the test setup. Nevertheless, for testing drilling incidents the flow loop produces realistic scenarios, only preceded by a full-scale test rig or actual drilling with logged incidents.

Figure 2: Stand pipe with pressure measurement p_p (left) and chokes with pressure measurement p_c (right).

3. Model-based fault detection and isolation

Fault diagnosis methods may be divided into model-based and data-based techniques [6]. Model-based methods are typically used if mathematical models of the process and faults are available, whereas data-driven methods use historical data of complex systems to determine occurring faults, see, e.g., [24]. Although complex, the drilling process is limited in size and can be divided into two subsystems separated by the drill bit. With a quite simple hydraulics model available, this paper uses a model-based diagnosis method, namely analytical redundancy relations to generate residuals, together with statistical change detection to detect changes to the residuals.

Model-based fault detection and isolation (FDI) is defined in [25] as

- *Fault detection:* Determination of the presence of a fault in the system.
- *Fault isolation:* Determination of the kind and location of the fault.

The FDI procedure can be divided into function blocks. A *residual generator* which provides signals that ideally deviate from zero only if a fault happens, and a *decision system* giving a hypothesis about which parts of the system are faulty [11], see Fig. 3.

Residuals in a model-based fault detection and isolation method can be generated using state estimation, parameter estimation, joint state and parameter estimation, or analytical redundancy relations, see, e.g., [26, 27]. Joint state and parameter estimation is achieved using an adaptive observer, or extending the state vector in a Kalman filter by relevant parameters. Adaptive observers for state and parameter estimation was the topic in [7, 8]. This paper focuses on using analytical redundancy relations. Benefits and drawbacks of the two methods are compared in Tab. 1, which is a shortened version of Tab. 14.1 in [28].

4. System representation

The model of the drilling process including system dynamics, algebraic equations, inputs, and measurements are presented in this section. Consider the system

$$\dot{x} = f(x, u, \theta), \tag{1a}$$

$$y = h(x, u, \theta), \tag{1b}$$

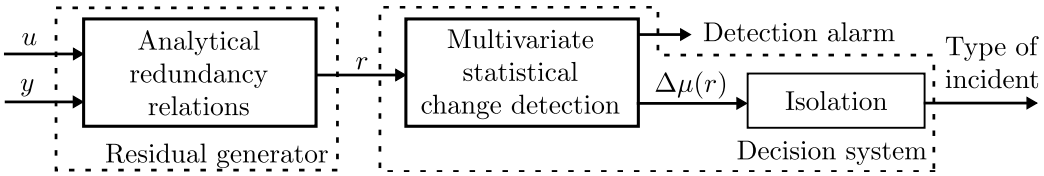

Figure 3: Fault detection and isolation using analytical redundancy relations to generate residuals r as a function of measured inputs u and outputs y. Changes in mean $\Delta\mu(r)$ are detected using statistical change detection, and incident type isolation is determined using change direction of the mean.

where $x \in \mathbb{R}^{n_x}$ is the state vector, $u \in \mathbb{R}^{n_u}$ is the input vector, and $\theta \in \mathbb{R}^{n_\theta}$ is a constant parameter vector. Each equation $\dot{x}_i = f_i(x, u, \theta)$, $y_i = h_i(x, u, \theta)$, and u_i in (1) will represent a constraint

$$c_i \in \mathcal{C} \tag{2}$$

in the constraint set $\mathcal{C}$, used in generating the analytic redundancy relations, as well as analyzing the relationship between the ARR and the faults.

The analytic redundancy relations are easily generated from simple model equations. In general, simple models give faster and easier real-time diagnostic classifiers [21], while unmodeled dynamics can be treated as model uncertainty. Motivated by this, the dynamics in the well is modeled with a modification of the simplified model from [29] for the drilling hydraulics,

$$(c_1): \ \frac{dp_c}{dt} = \frac{\beta_a}{V_a}(q_p - q_c) \tag{3a}$$

$$(c_2): \ \frac{dq_p}{dt} = \frac{1}{M}((\rho_a - \rho_d)gh + p_c - p_p + \theta_d q_p^2 + \theta_b q_p^2 + \theta_a q_p^2) \tag{3b}$$

where p_p is the pressure at the pump, p_c the pressure upstream the choke, q_p the pump flow and q_c flow through the choke, see Fig. 1. The pressure drop $p_{\Delta c}$ over the choke is measured by a dedicated pressure difference sensor. The parameters β_a and V_a represent the bulk modulus and volume of the annulus, respectively, and M is the integrated density of the total liquid in the drillstring and the annulus per cross section area. The density of the fluid in the annulus is ρ_a, and ρ_d in the drillstring, g is the gravitational acceleration, and h is the depth of the well. The pressure dynamics in the drillstring is ignored, assuming in (3) that the flow q_p from the rig pump equals the flow through the bit. This pressure dynamics is typically orders of magnitude faster than the occurring incidents, making the assumption valid.

Table 1: Comparison of combined state and parameter estimation with analytical redundancy relations for fault diagnosis, with the preferred method highlighted. Adapted from [28].

Characteristics	**Combined state and parameter estimation**	**Analytical redundancy relations**
Fast detection	Relatively fast, dependent on tuning	*Fast*
Detecting and isolating sensor and actuator bias	Dependent on model and setup	*Inherent*
Estimation of fault magnitude	*Possible, but dependent on model and setup*	Requires additional estimation
Propagation of measurement noise	*Dependent on tuning*	Needs to be handled if measurement differentiation is required
Design of method	Dependent on model, may require expert knowledge to derive observer	*Straightforward if tools are available*
Model parameters	*Unknown, time-varying*	Known, constant
Excitation requirements	Possibly	*No*

The friction through the system is modeled using a turbulent friction relationship $\theta_i q_b^2$ for the drillstring, bit, and annulus, respectively with $i \in \{d, b, a\}$. As shown in [8], this relationship matches the flow loop data well. For laminar flow, a linear relationship can be applied. The friction coefficients θ_i can be found offline using some form of parameter identification, while all other parameters are assumed constant and known.

The algebraic equations of friction and choke flow are given by

$$(c_3): \ p_d = p_p - \theta_d q_p^2 + \rho_d g h, \tag{3c}$$

$$(c_4): \ p_a = p_d - \theta_b q_p^2, \tag{3d}$$

$$(c_5): \ p_a = p_c + \theta_a q_p^2 + \rho_a g h, \tag{3e}$$

$$(c_6): \ q_c = g_c(u_c)\sqrt{p_{\Delta c}}, \tag{3f}$$

where p_a is the pressure in the annulus, downstream the bit. This pressure is commonly named the *bottomhole pressure*. The pressure upstream the bit is denoted p_d. The choke opening input constraint is

$$(c_7): \ u = u_c, \tag{3g}$$

and the measurements are

$$(c_8 - c_{14}): \; y = \begin{bmatrix} p_p, & p_d, & p_a, & p_c, & p_{\Delta c}, & q_p, & q_c \end{bmatrix}^\top. \tag{3h}$$

Note that both states p_c and q_p in (3) are measured, as well as the downhole pressures p_a and p_d. In the following sections these downhole sensors are first assumed available. Analysis and discussion of the case without the downhole sensors follows subsequently.

5. Analytical redundancy relations

Analytical redundancy relations (ARR) are functions of the system inputs and outputs and their derivatives, and can be used to derive nonlinear residuals [10]. Analytical redundancy in fault diagnosis can be used to check for inconsistencies between the actual system and the system model, and residuals can be used for fault detection and isolation [21]. The residuals should be (close to) zero during the fault free case, and significantly non-zero during a fault. Detection of change from zero to non-zero of the residuals can then be used for fault detection and isolation.

The residuals designed based on system (1) can be written as

$$r(\bar{y}^{(q)}, \bar{u}^{(q)}, \theta) = 0, \tag{4}$$

where $\bar{y}^{(q)}$ and $\bar{u}^{(q)}$ are vectors of y and u and their time derivatives up to order q, respectively, see, e.g., [10, 11, 30, 31]. In case of measurement noise, the residuals (4) are not identically zero in the fault-free case. Thus, a fault is detected using hypothesis testing by differentiating between the *null hypothesis* $\mathcal{H}_0$, and the *alternative hypothesis* $\mathcal{H}_1$,

$$\mathcal{H}_0: \quad r(\bar{y}^{(q)}, \bar{u}^{(q)}, \theta) = w, \tag{5}$$

$$\mathcal{H}_1: \quad r(\bar{y}^{(q)}, \bar{u}^{(q)}, \theta) = A + w, \tag{6}$$

where w is white noise with probability distribution $f(x; \Pi)$ with statistical parameters Π, and where $A \neq 0$ is representing the effect of the fault. Computing ARR is done by eliminating the state in the system equations. Different tools and methods available for generating ARR and *minimal structurally overdetermined sets* [30, 11, 32] for residuals are compared in [33]. The MATLAB toolbox SaTool [34] comprises algorithms to find complete matchings between the constraints and the unknown system variables, and is used to generate the residuals in this paper.

5.1. ARR for the drilling model

From the system constraints defined in (3), the Matlab tool SaTool is used to find the following residuals,

$$r_1 = \frac{d}{dt}y_4 - \frac{\beta_a}{V_a}(y_6 - y_7), \tag{7a}$$

$$r_2 = \frac{d}{dt}y_6 + \frac{1}{M}\left((\rho_a - \rho_d)gh - y_1 + y_4 + \theta_a y_6^2 + \theta_b y_6^2 + \theta_d y_6^2\right), \tag{7b}$$

$$r_3 = \theta_d y_6^2 - \rho_d gh - y_1 + y_2, \tag{7c}$$

$$r_4 = \theta_b y_6^2 - y_2 + y_3, \tag{7d}$$

$$r_5 = \theta_a y_6^2 + \rho_a gh - y_3 + y_4, \tag{7e}$$

$$r_6 = y_7 - g_c(u_c)\sqrt{y_5}, \tag{7f}$$

which will be used for fault detection and isolation.

Differentiating a signal with noise leads to obvious challenges. A common procedure to reduce noise is to low-pass filter the signal, in this case the residuals. However, if the residuals are low-pass filtered the result will be slower detection. Furthermore, since both of$y_6(t)$ and dy_6/dt appear in r_2, the derivative of the signal is not needed for detectability nor isolability and the presence of $y_6(t)$ ensures that a change in y_6 is strongly detectable. With respect to dy_4/dt, $y_4(t)$ itself appear in r_2 and r_5, which assures strong detectability and isolability. Therefore, the derivatives of $y_4(t)$ and $y_6(t)$ in (7) are not needed and they are omitted in the further analysis and application. This is equivalent to considering the algebraic version of constraints c_1 and c_2 in (3), that follow with $dy_4/dt \equiv 0$ and $dy_6/dt \equiv 0$. Rapid changes do not take place in the normal drilling operation, and the derivatives would be within the noise floor.

An exception is a so called connection, which is the operation of adding a new drillpipe to the drillstring. In this case, the flow rate is ramped down, then up again after a complete connection. If, nevertheless, dy_6/dt should change rapidly, r_2 might give a short deviation from zero but $[r_1, r_3, r_4, r_5]^T \simeq \mathbf{0}$, so a $\mathbf{H}_1$ hypothesis would be rejected. If dy_4/dt should change rapidly, r_2 would deviate for a short while, but since none of the other residuals would deviate from zero, a false $\mathbf{H}_1$ alarm would be rejected, also in this case. Furthermore, this operation is known and can be accounted for in a monitoring system.

5.2. Relations between faults in analytic and structural domains

In the structural domain, we consider violations of normal behaviors and analyze the ability to detect whether a violation has happened. Isolation in this domain means to determine which constraint has been violated. When translating to the analytic domain, residuals (7) are expressed as functions of measured signals y, of input u, and of process parameters in θ, ρ, V_a, etc.

5.3. ARR and constraint dependency

The matching between residuals (7) and constraints (3) was found using the ranking algorithm implemented in SaTool [34]. Subsequent calculation of the analytical redundancy relations is achieved by expressing that $c_k = 0$ is an ARR when c_k is an unmatched constraint, i.e., redundant in the calculation of the unknown variables but valid and useful as a test quantity. With c_k being a function of the variables in the system and with all unknown variables being calculable as prescribed by the complete matching, a backtracking along the path found by the matching will lead to c_k being a function expressed solely by known variables. The calculation of c_k will be a function also of the constraints c_i along the paths of the backtracking.

As a next step, the ARR $c_i = 0$ is replaced by the test quantity $r_j = c_i$ where r_j is a residual. The resulting dependencies between the constraints and the residuals are listed in Tab. 2. An 'X' in the table at position (j, i) means that a constraint c_i is used in the calculation of residual r_j. A violation of c_i will therefore influence r_j such that the function $r_j(t)$ will be nonzero for some or all t after $c_i(t) \neq 0$ has happened. This is referred to as *detectability*. *Isolability* means that it is possible to determine which particular constraint was violated. Precise definitions can be found in [11].

Table 2: Dependency matrix between residuals and constraints.

	c_1	c_2	c_3	c_4	c_5	c_6	c_7	c_8	c_9	c_{10}	c_{11}	c_{12}	c_{13}	c_{14}
r_1	X										X		X	X
r_2		X						X			X		X	
r_3			X					X	X				X	
r_4				X					X	X			X	
r_5					X					X	X		X	
r_6						X	X					X		X

Tab. 3 shows structural detectability and isolability of each constraint using the residuals r. *Structural detectability*, denoted d, follows if the corresponding column i in Tab. 2 is non-zero, i.e., comprises an 'X'. *Structural isolability*, denoted i, requires that the signature in column i in Tab. 2 differs from the signature of all other columns. Constraints c_6, c_7 and c_{14} are only detectable, denoted 'd' in Tab. 3. This means that it is not possible to distinguish between a violation of these three constraints or, in other words, that it is not possible to distinguish between faults in sensors q_c, $p_{\Delta c}$ and choke opening u_c. This can be also seen in the constraint dependency table shown in Tab. 2, giving the same matching for r_6 with c_6, c_7 and c_{12}. Fortunately, all these sensors are topside and easily available. If a low reliability is experienced in these sensors, redundant sensors could be installed to enhance isolability. Pressure sensors in particular are quite small and easy to install.

Table 3: Detectability and isolability of constraints.

c_1	c_2	c_3	c_4	c_5	c_6	c_7	c_8	c_9	c_{10}	c_{11}	c_{12}	c_{13}	c_{14}
i	i	i	i	i	d	d	i	i	i	i	d	i	i

Localization of the position of an incident, which was done in [8] based on parameter and state estimation, would also be possible using ARR by including additional measurements in the annulus and extending the model (3) to include friction parameters representing friction between the measurements. However, this will lead to quite many constraints and residuals. To narrow down the scope of this paper, localization is omitted in the fault diagnosis, focusing on incident detection and type isolation.

5.4. Fault isolation with analytical redundancy relations

The faults are not modeled explicitly in (3). This has been done for mechanical systems in, e.g., [35], where faults in an automotive engine were modeled explicitly. This would result in a mapping between the faults and the residuals. In this paper, this relationship is implicit, and a physical change to the process will affect the residuals as indicated in Tab. 2 as a match between residual r_j and constraint c_i.

The challenge with explicit modeling of the faults lies both in the nature of some of the faults and the difficulty of modeling any possible incident or fault. The methodology of [35] is aimed at isolating only the specific fault

included in the model. The generic approach used here will be sensitive to any deviation from the normal behavior that was described by (3).

A drillstring washout, a loss of circulating drilling fluid, or an influx will change the flow in parts of the process. However, the position of the fault is unknown, and therefore difficult to implement in the model. The different faults and sensor bias drifts are listed in Tab. 4. An 's' in Tab. 4 denotes *strong detectability* of the corresponding fault (as opposite to weak detectability), meaning that the affected residual reaches a non-zero steady state, see, e.g., [11].

The incidents are defined as:

- A *drillstring washout* (f_{wo}) is a leakage from the drillstring to the annulus, and will reduce flow in the lower parts of the system. This will be seen as a reduced friction loss in the drillstring, over the bit, and in the annulus.

- *Lost circulation* (f_{ls}) of drilling fluid to the reservoir will reduce friction in the annulus.

- An *influx* (f_{in}) of reservoir fluids will have an opposite effect as lost circulation giving larger flow out of the well than in, and an increased friction in the annulus.

- A *plugging of the drill bit nozzles* (f_{bp}) will cause an increased pressure drop over the drill bit. This will then give a higher back-pressure at the bit, giving increasing values of pump pressure and upstream bit pressure.

- A *pack-off* (f_{po}) is a partial or fully plugging of of solids around the drillstring in the annulus, giving increased pressure drop in this section. It will therefore behave similar as a bit nozzle plugging, but with an increased friction drop in the annulus rather than over the bit.

- A *choke plugging* (f_{cp}) is a partially or fully blocking of the MPD choke, caused by formation solids. This will change the characteristics of the choke.

- Bias drifts in pressure sensors p_p, p_c, p_d and p_a are denoted as Δp_i for sensor p_i for a positive drift.

All the sensor faults and process incidents are possible to isolate, as seen in Tab. 4, except from a negative bias drift in choke pressure ($-\Delta p_c$) and a pack-off (f_{po}) which have the same signature. Note that the method does not necessarily handle isolation of simultaneous incidents. However, for drilling this is not considered a limitation, since each of the incidents are quite severe. If an incident is detected and isolated, drilling should be suspended and appropriate actions should be taken immediately to reduce possible consequences.

Table 4: Fault dependency table with downhole measurements. Strong detectability is denoted 's'.

	Δp_p	Δp_c	Δp_d	Δp_a	f_{wo}	f_{ls}	f_{in}	f_{bp}	f_{po}	f_{cp}
r_1						$-$	$+$			
r_2	$-$	$+$			$+$	$+$	$+$	$-$	$-$	
r_3	$-$		$+$		$+$					
r_4			$-$	$+$	$+$			$-$		
r_5		$+$		$-$	$+$	$+$	$-$		$-$	
r_6										$-$
	s	s	s	s	s	s	s	s	s	s

5.5. Analytical redundancy relations with only topside measurements

Analysis up until now assumed available downhole pressure sensors through a wired drill pipe. However, this is a novel technology without a large user base in operating drilling rigs. More commonly, only a single downhole pressure sensor is available, with high latency, low bandwidth transmission and with a relatively high rate of downtime. In many cases no downhole measurement is available at all. It is hence interesting to investigate what can be done using only topside measurements, in other words, not using p_d and p_a in the measurement vector (3h).

Conducting the same analysis as before, but removing p_d and p_a from (3),

the alternative residuals $\tilde{r}$ are

$$\tilde{r}_1 = \frac{d}{dt}\tilde{y}_2 - \frac{\beta_a}{V_a}(\tilde{y}_4 - \tilde{y}_5), \tag{8a}$$

$$\tilde{r}_2 = \frac{d}{dt}\tilde{y}_4 + \frac{1}{M}\left((\rho_a - \rho_d)gh - \tilde{y}_1 + \tilde{y}_2 + \theta_f \tilde{y}_4^2\right), \tag{8b}$$

$$\tilde{r}_3 = \tilde{y}_2 - \tilde{y}_1 + \theta_f \tilde{y}_4^2, \tag{8c}$$

$$\tilde{r}_4 = \tilde{y}_5 - g_c(u_c)\sqrt{\tilde{y}_3}, \tag{8d}$$

the topside measurements are

$$\tilde{y} = \begin{bmatrix} p_p, & p_c, & p_{\Delta c}, & q_p, & q_c \end{bmatrix}^\top, \tag{9}$$

and

$$\theta_f = \theta_d + \theta_b + \theta_a \tag{10}$$

is the friction coefficient of the total friction from pump to choke, represented by the parameter θ_f. Since no downhole measurements are available, θ_d, θ_b and θ_a are not possible to identify individually.

Table 5: Fault dependency table with no downhole measurements. Strong detectability is denoted 's'.

	Δp_p	Δp_c	f_{wo}	f_{ls}	f_{in}	f_{bp}	f_{po}	f_{cp}
$\tilde{r}_1$				$-$	$+$			
$\tilde{r}_2$	$-$	$+$	$+$	$+$	$+$	$-$	$-$	
$\tilde{r}_3$	$-$	$+$	$+$	$+$	$+$	$-$	$-$	
$\tilde{r}_4$								$-$
	s	s	s	s	s	s	s	s

With a possibility of both positive and negative drift of the pressure sensors, it is not possible to separate washout (f_{wo}), bit nozzle plugging (f_{bp}) and pack-off (f_{po}) from bias drift, as seen in Tab. 5, although subgroups of sensor faults and physical incidents can be isolated. This is as expected, since drillstring washout, bit nozzle plugging and pack-off only change the pressure drop seen from pump to choke, without changing flow rate. Without downhole measurements, it is difficult to separate these from bias drift. However, since the measurements are located topside, they are more easily accessible than downhole measurements. One could install redundant pressure sensors

making it easy to isolate a sensor with bias drift and exclude it from the diagnostic algorithm. Drillstring washout could then be isolated from either a bit nozzle plugging or a pack-off.

6. Multivariate change detection and change direction for FDI

Detecting changes to the residuals are done by using a multivariate generalized likelihood ratio test (GLRT). By using a multivariate scheme, changes to all residuals are considered jointly. For diagnosis based on change detection in [7], this approach was found to be superior compared with using independent univariate tests on each signal.

It is common to assume that the noise is Gaussian distributed. However, noting that the residuals are sums of pressure measurements, and squares of flow measurements, residuals are not likely to be Gaussian. The distribution is checked using a Kolmogorov-Smirnov test for the Gaussian, Student t, Laplace, and Cauchy distributions in Tab. 6, showing a high p-value for all residuals with the t-distribution, which furthermore is the only distribution with all p-values above 0.05, a typical statistical threshold. To save space, only the p-values for the lost circulation case is shown, but the t-distribution is well suited for all cases. Non-Gaussian distributions on estimated parameters and residuals are studied in [7, 8, 36, 37].

Table 6: Kolmogorov-Smirnov test of the residuals r for the lost circulation case at $\mathcal{H}_0$, with p-values above 0.05 highlighted.

Residual	Gaussian	Student t	Laplace	Cauchy
r_1	**0.064**	**0.79**	**0.059**	1.0×10^{-6}
r_2	0.034	**0.70**	0.010	1.5×10^{-7}
r_3	2.8×10^{-9}	**0.76**	**0.75**	5.6×10^{-3}
r_4	$< 10^{-12}$	**0.87**	**0.053**	0.048
r_5	0.0031	**0.99**	0.0011	4.6×10^{-7}
r_6	0.0082	**0.19**	3.2×10^{-7}	4.2×10^{-10}

The detection problem of change in a signal x is to distinguish between the *null hypothesis* $\mathcal{H}_0$ and the *alternative hypothesis* $\mathcal{H}_1$, which can be presented as

$$\mathcal{H}_0 : \quad x \sim \mathcal{D}(\Pi_0; \mathcal{H}_0), \tag{11a}$$

$$\mathcal{H}_1 : \quad x \sim \mathcal{D}(\Pi_1; \mathcal{H}_1), \tag{11b}$$

where x has the probability distribution $D(\Pi_i; \mathcal{H}_i)$ with statistical parameters Π_i under hypothesis $\mathcal{H}_i$.

6.1. Generalized likelihood ratio

The window limited generalized likelihood ratio of signal $x(k)$ with noise distributed by probability density function $f(x;\Pi)$, and with statistical parameters Π, is given by

$$g(k) = \max_{k-N+1\leq j\leq k-\tilde{N}} \ln \frac{\prod_{i=j}^{k} f(x(i);\Pi_1)}{\prod_{i=j}^{k} f(x(i);\Pi_0)}, \tag{12}$$

where Π_0 denotes statistical parameters during the $\mathcal{H}_0$ hypothesis, and Π_1 during the $\mathcal{H}_1$ hypothesis. The window is given by $0 \leq \tilde{N} \leq N$, and is used to reduce computational cost [**?**].

The p-variate t-distribution of a vector signal x with mean μ, correlation S, and degrees of freedom ν is

$$f(x;\mu,S,\nu) = \frac{\Gamma((p+\nu)/2)}{\Gamma(\nu/2)(\pi\nu)^{p/2}|S|^{1/2}} \left[1+\frac{1}{\nu}(x-\mu)^\top S^{-1}(x-\mu)\right]^{-\frac{p+\nu}{2}}, \tag{13}$$

where $\Gamma(z)$ is the Gamma function. Note that μ is the mean of x when $\nu > 1$ [38]. The corresponding GLRT statistic was derived in [7] for a change in mean μ from μ_0 to μ_1 with S and ν constant, and was shown to be

$$g(k) = \max_{k-N+1\leq j\leq k-\tilde{N}} \frac{p+\nu}{2} \sum_{i=j}^{k} \left[-\ln\left(1+\frac{1}{\nu}(x(i)-\hat{\mu}_1)^\top S^{-1}(x(i)-\hat{\mu}_1)\right) + \ln\left(1+\frac{1}{\nu}(x(i)-\mu_0)^\top S^{-1}(x(i)-\mu_0)\right)\right], \tag{14}$$

where $\hat{\mu}_1$ is the maximum likelihood ratio of the mean after change,

$$\hat{\mu}_1 = \frac{1}{k-j+1}\sum_{i=j}^{k} x(i). \tag{15}$$

6.2. Fault isolation by determining change direction of the residuals

The GLRT statistic (14) is scalar, and an estimate of the magnitude of change is provided by (15). To determine the type of fault, the direction of change can be considered, which was done for parameter estimation in [7] and [8], and is similar to [20] where the direction of change of residuals was considered.

Problem 1 (Fault detection)**.** *Given a sampled time sequence of vectors of residuals $r(k)$, with change from known condition $r_0(k)$ to unknown $r_1(k)$. Define the index set $\mathbb{N}_N := \{i \in \mathbb{N} : 1 \leq i \leq N\}$ and let $i_f \in \mathbb{N}_{N_f}$ be the possible fault indices. Let a fault signature matrix be D, with column vector D_i corresponding to fault index i_f. Then distinguish between two hypotheses*

$$\mathcal{H}_0 : \quad r(k) = 0 + w(k), \qquad \textit{no fault present,} \tag{16a}$$

$$\mathcal{H}_1 : \quad r(k) = D_i v(k) + w(k), \qquad \textit{a fault is present.} \tag{16b}$$

Problem 2 (Fault isolation)**.** *Given that $\mathcal{H}_1$ has been accepted, determine that a particular fault i_f^* is present of the possible faults $i_f \in \mathbb{N}_{N_f}$, by determining the best fit of* (16b) *for the different fault types.*

The matrix D is constructed based on Tab. 4, where each fault type in the table corresponds to one column vector D_i. An element with '$-$' in the table gives a value of -1 in D, '+' gives a value of 1, and 0 is used otherwise. Negative bias drift is isolated using changed signs for the corresponding positive drift.

The fault type i_f^* is isolated using a projection of the change in mean $\hat{\mu}_1 - \mu_0$ of the residual r onto the different column vectors D_i corresponding to different faults, finding the largest projection,

$$i_f^* = \arg\max_i \frac{D_i^\top (\hat{\mu}_1 - \mu_0)}{D_i^\top D_i}. \tag{17}$$

6.3. Deciding on threshold value for the GLRT statistic

By finding the distribution of the test statistic $g(k)$ at $\mathcal{H}_0$, a threshold value h can be chosen with a desired probability of false alarm P_{FA}. If test statistic data is available at $\mathcal{H}_1$, the probability P_D of detecting a fault may also be found. An asymptotic distribution may be estimated from data. A Weibull distribution was fitted to the the test statistic of the residuals in [36] and estimated parameters in [7, 8]. A lognormal distribution is used in [39].

The test statistic data of r for the influx case at $\mathcal{H}_0$ is plotted in Fig. 4, showing a good fit of the tail to the Weibull distribution. The lognormal distribution gives a good fit overall, but not of the last 10 % of the tail, which is the part of the distribution that is most important for threshold selection. The Weibull distribution is applied for all cases to determine the threshold h of $g(k)$.

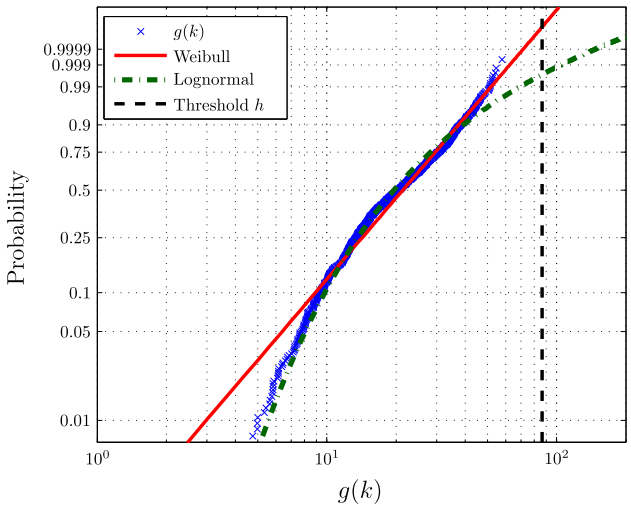

Figure 4: Weibull probability plot of $g(k)$ at $\mathcal{H}_0$ for the influx case. Test statistic data fitted to Weibull distribution (red solid line) and lognormal distribution (green dashed dotted line). The threshold h is calculated from a fitted Weibull distribution with $P_{FA} = 10^{-6}$, plotted as a vertical black dashed line.

The Weibull distribution has the probability density function $f(x;\alpha,\beta)$ and cumulative distribution $F(x;\alpha,\beta)$ given by

$$f(x;\alpha,\beta) = \frac{\beta}{\alpha}\left(\frac{x}{\alpha}\right)^{\beta-1} e^{-(x/\alpha)^{\beta}}, \quad x \geq 0, \tag{18}$$

$$F(x;\alpha,\beta) = 1 - e^{-(x/\alpha)^{\beta}}, \quad x \geq 0, \tag{19}$$

where $\alpha > 0$ is the scale parameter and $\beta > 0$ is the shape parameter. The inverse cumulative distribution can be used to determine the threshold h as a function of the probability of false alarms P_{FA}, even if the residuals are not independent and identically distributed [39, 40, 41]. The threshold is then given by

$$h = Q(1 - P_{FA}; \mathcal{H}_0, \alpha_0, \beta_0) = \beta_0 \left(-\ln(P_{FA})\right)^{1/\alpha_0}, \tag{20}$$

where α_0 and β_0 are the parameters of the Weibull distribution fitted to $g(k)$ under $\mathcal{H}_0$. If $\mathcal{H}_1$ data is available, the probability of detecting a fault P_D is given as a function of the threshold h,

$$P_D = 1 - F(h; \mathcal{H}_1, \alpha_1, \beta_1) = e^{-(x/\alpha_1)^{\beta_1}}, \tag{21}$$

where α_1 and β_1 are the statistical parameters of the test statistic at $\mathcal{H}_1$.

7. FDI of flow loop data using downhole measurements

Fault detection and isolation of different incidents in data from the flow loop tests is done using the methods described in Secs. 5 and 6. This section presents fault detection and isolation where downhole measurements are available. The cases studied are lost circulation, gas influx, bit nozzle plugging, choke plugging, and a positive bias drift in the downhole sensor p_a. The measured pressure and flow rates are plotted in Fig. 5, which are sampled at 10 Hz. The plot shows a concatenation of different test cases recorded over a time period of several weeks, and are not necessarily plotted in chronological order. In the test setup some of the incidents are also measured, used only as ground truth about the time interval and magnitude of the incident, and shown in Fig. 6. Note that bit nozzle plugging and choke plugging occurring during the interval 40 to 60 minutes are not measured.

The residuals r given by (7) are plotted in Fig. 7 for all five cases of incidents. The physical parameters of the flow loop are found using available information about the drilling process and are listed Tab. 7. The friction parameters θ_a, θ_b and θ_d in (7) are found using an off-line parameter estimation method. The parameters are assumed constant or varying much slower than the dynamics in the process, and thus kept constant in r. In this case the parameters are found using the adaptive observer in [42] of data $\mathcal{H}_0$ known to be fault free. Since the flow-loop setup was used extensively for a various number of tests, many not included in this paper, there are some differences between the cases, giving slightly different friction parameters, representing natural variation during operation.

Table 7: Physical flow loop parameters.

β_a	$2.2 \times 10^9\,\mathrm{Pa}$	Effective bulk modulus
ρ_d, ρ_a	$1000\,\mathrm{kg/m^3}$	Drilling fluid density
M_a	$3.74 \times 10^7\,\mathrm{Pa\,s^2/m^3}$	Integrated density per cross section
V_a	$13.2\,\mathrm{m^3}$	Volume of fluid in annulus
h	$2.14\,\mathrm{m}$	Depth of well at bit
L_d, L_a	$700\,\mathrm{m}$	Length of drillstring/annulus

From Fig. 7 it is apparent that different faults affect the residuals in some manner, giving non-zero values. However, due to measurement noise, these changes are very difficult to detect reliably without some change detection method. The methods in Sec. 6 are used for fault detection and isolation

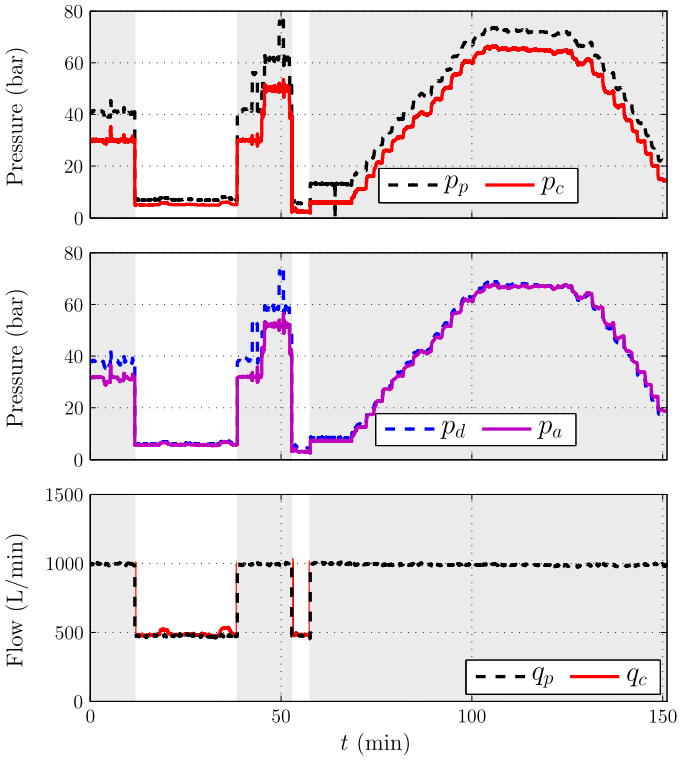

Figure 5: Topside pressure measurements (top), downhole pressure measurements (middle), and flow measurements (bottom) of the five cases of lost circulation, gas influx, bit nozzle plugging, choke plugging, and positive bias drift in sensor p_a. The different cases are separated with alternating grey and white backgrounds. There is significant noise in the data.

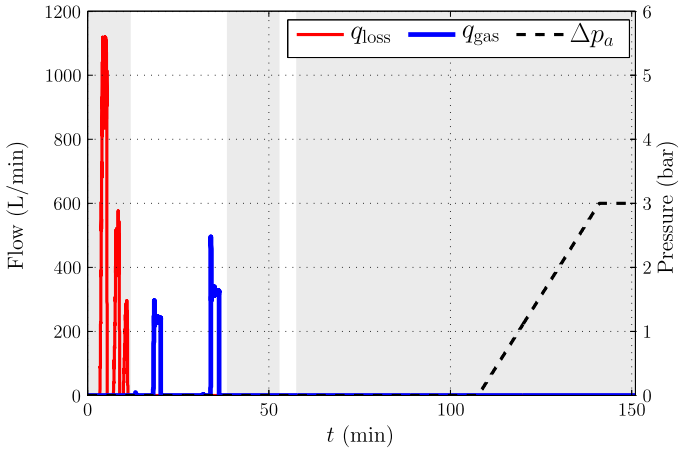

Figure 6: Downhole incidents of lost circulation and gas influx in the first 40 minutes of data. Bit nozzle plugging and choke plugging from 40 to 60 minutes are not measured. Artificially added bias drift in p_a starts at 110 minutes. None of this information is available to the diagnosis method.

in the different cases described in the following subsections. For all cases a window length of

$$N = 200 \tag{22}$$

samples is used, corresponding to 20 seconds and is considered sufficiently long. A too short window length decreases the detection rate, whereas an increasing window length increases the computational cost. Choosing a sufficiently long window length was discussed in [8]. A probability of false alarm

$$P_{FA} = 10^{-6} \tag{23}$$

is used to determine thresholds, which corresponds to an expected false alarm rate of 0.00018 per hour (under 2 per year). Due to process disturbances, there has been used an additional requirement that an alarm is set off only if 200 samples (20 s) of $g(k)$ is above the threshold. The spikes in residuals r_2 and r_3 happening at 64 minutes are caused by a 2 second temporal artifact in p_p.

7.1. Lost circulation

The first case studied is lost circulation of drilling fluid to the reservoir, which is labeled as fault f_{ls} in Tab. 4. From this table, loss of drilling fluid is detected and isolated if $g(k)$ is above the threshold, and that the mean of

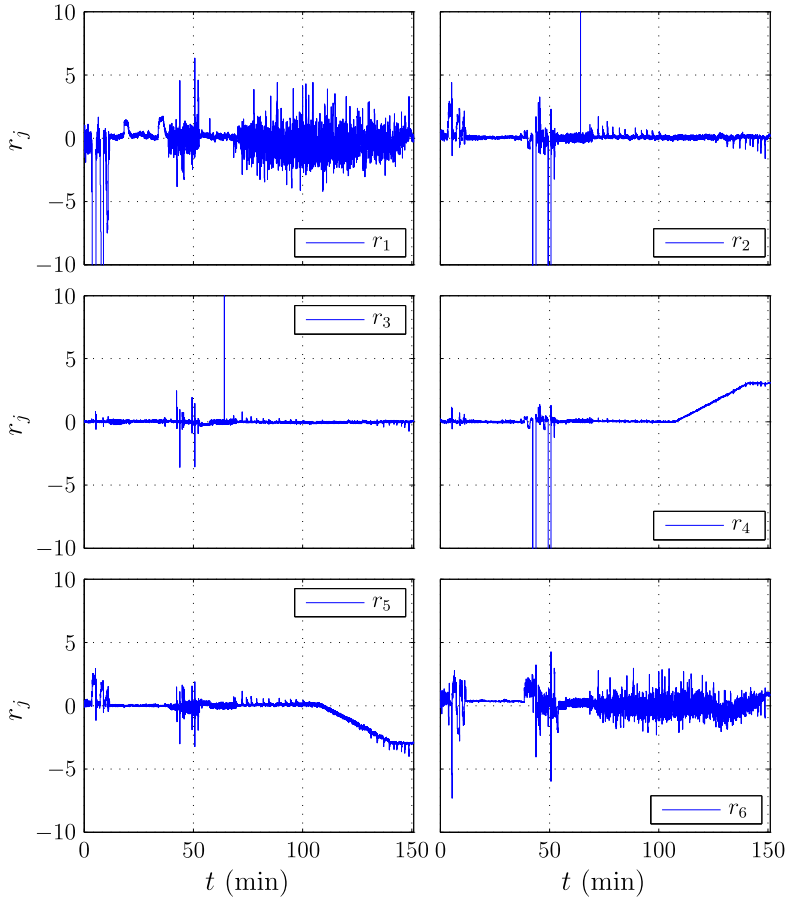

Figure 7: Residuals r_1 - r_6 for lost circulation, gas influx, bit nozzle plugging, choke plugging, and positive bias drift in sensor p_a, using downhole measurements.

r is changing in a negative direction for r_1, and positive direction for r_2 and r_5. Three different loss rates are tested with different magnitude, plotted in red in Fig. 6. The first loss is at over 1000 L/min, which is a complete loss of drilling fluid. The last one is around 250 L/min, or 25 % of circulation rate. All three loss rates are quite large, and as expected, detection and isolation are quite manageable. Fault detection is shown in the upper panel of Fig. 8, showing a value of $g(k)$ above threshold for all three losses. The actual loss intervals are shown in grey in the lower panel, where fault isolation is correctly achieved using change direction of r, shown in blue.

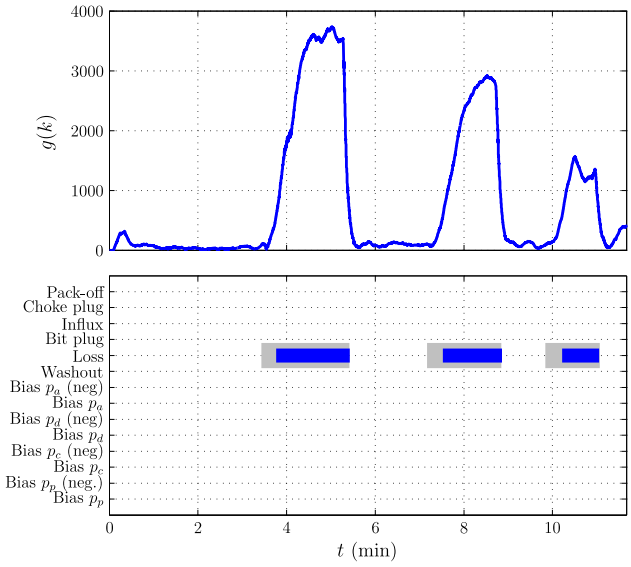

Figure 8: Detection and isolation of lost circulation. Actual loss shown in grey.

7.2. Gas influx

Gas influx is a complex case to correctly diagnose. When gas enters the annulus, the dynamics changes drastically from single-phase to multi-phase flow. Limitations of the model (3) during an influx is discussed in [8], where the model is not well suited to determine information about the gas influx once it has entered the annulus. However, detecting and isolating the initial occurrence of an influx is still possible, by determining change in the total annular friction and change in the flow rate difference in and out of the well. The procedure once an influx is detected is to shut in the well, which is done by closing the blow-out preventer (BOP) around the

drillstring, blocking annular flow. It is therefore still possible to use the method described in this paper. Two influxes of gas in the annulus are plotted in blue in Fig. 6. Corresponding detection is shown in Fig. 9. Both influxes are correctly detected and isolated. However, after the first influx, the gas is transported through the annulus, giving different dynamics and friction. This gives some incorrectly isolated incidents, while most are correctly isolated as gas in the system. Nevertheless, as discussed above, once the first influx is detected and isolated the drilling crew will most probably decide to shut in the well and remove the gas in the system by circulating a heavier drilling fluid.

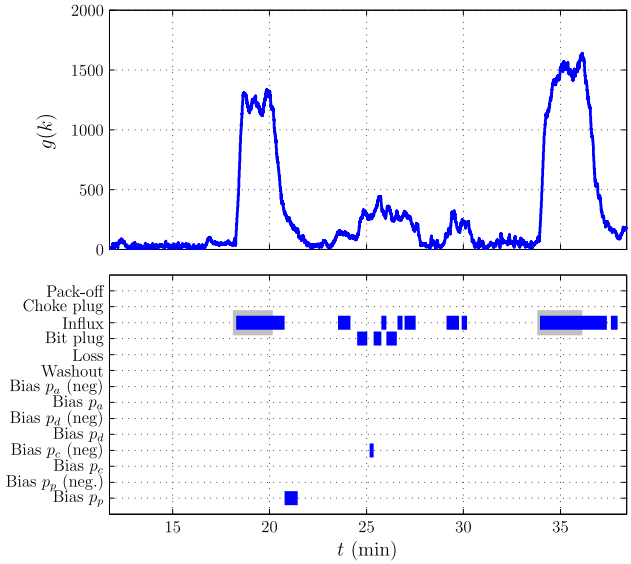

Figure 9: Detection and isolation of two influxes of gas into the well. Note that there is gas in the well also after injection. Some of it is correctly isolated as gas, some incorrectly as a bit nozzle plugging.

7.3. Plugging of drill bit nozzles

Plugging of the drill bit nozzles is not as severe as formation fluid influx and lost circulation, since the pressure in the well is not affected. Nevertheless, monitoring of the bit status is important in order to maintain drilling. A partial blocking of the nozzles will be seen as a higher pressure in the drillstring, which the operator has great benefits of determining the cause of. A full blocking of the nozzles will stop circulation of drilling fluid, halting progress.

Four pluggings of the bit nozzles are successfully detected and isolated in Fig. 10, two small and two large. Detecting a bit nozzle plugging may be possible by directly measuring the pressure drop over the bit, $p_d - p_a$. However, this pressure drop is a function of flow. In addition, changes to pressure measurements may be caused by other incidents. Thus is a complete diagnosis method favorable for distinguishing nozzle plugging from other incidents.

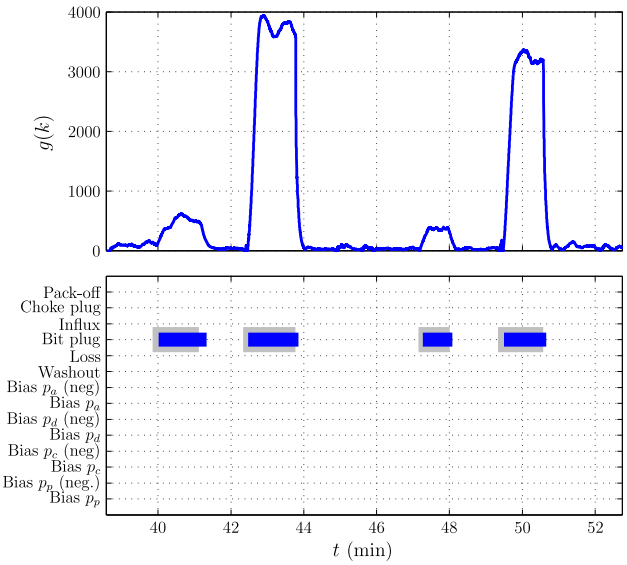

Figure 10: Detection and isolation of a plugging of the drill bit nozzles.

7.4. Plugging of MPD choke

If the choke in a managed pressure drilling operation becomes partially plugged, control of the back-pressure may be difficult. This pressure will directly affect the downhole pressure, which should be controlled within a pressure window. If the pressure is too low the well can start to produce, causing influxes, while a too high pressure may cause damage to the formation, which may result in lost circulation due to cracks in the formation.

Detection and isolation of a partial plugging of the MPD choke is shown in Fig. 11. The partial plugging is simulated in the flow loop as partially closing a dedicated valve upstream the choke. The plugging occurs in the very beginning of the recorded data set, and is correctly detected and isolated.

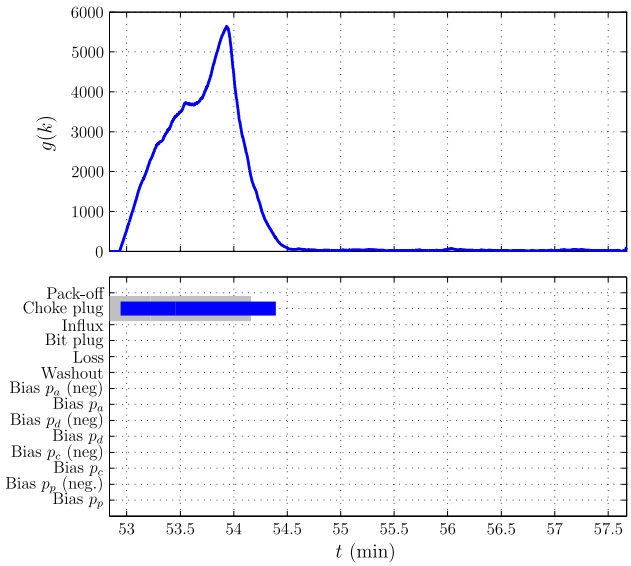

Figure 11: Detection and isolation of a plugging of the MPD choke.

7.5. Bias drift in bottomhole pressure sensor p_a

The four previous cases describe incidents which are physical changes in the process due to some induced physical incidents. Detection and isolation is based on residuals which again are functions of measurements of process variables and actuators. For such a method to be successful, the measurements must be reliable. In real life, uncertainty in measurements, such as bias drift, affects the diagnosis method. It is therefore important to also detect and isolate such effects.

In this case a positive drift in the downhole pressure sensor p_a is tested. The bias drift is artificially added to the pressure signal as a ramp function from 0 to 3 bar, starting at around 110 minutes in Fig. 6. This is occurring simultaneously as the choke opening is ramped up, giving a significant increase in choke pressure p_c, and thus also in p_d, p_a and p_p, shown in Fig. 5. Diagnosis of the bias drift is shown in Fig. 12, with an early detection of the drift where the bias is quite small. Determining that a bias drift is occurring from the measurements directly would be difficult for an operator, while it is successfully detected and isolated with the methodology in this paper.

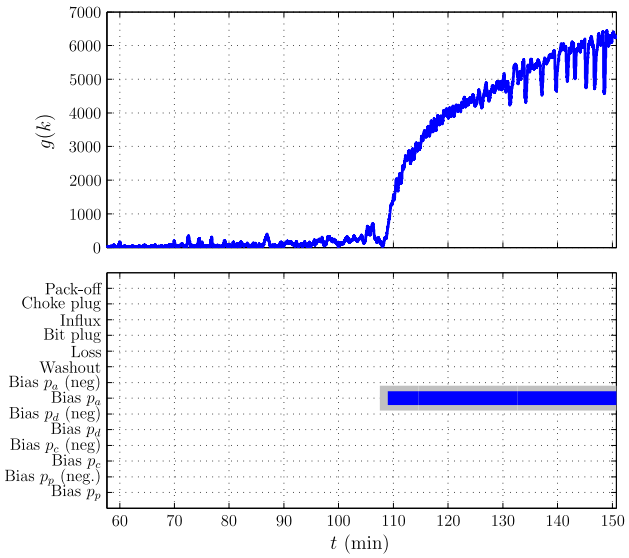

Figure 12: Detection and isolation of a positive bias drift in pressure sensor p_a.

8. FDI of flow loop data with only topside measurements

All cases in the previous section utilized downhole pressure sensors available when wired drill pipe technology is at hand. However, in most drilling rigs only a few downhole sensors are available, if any. This section investigates to what extent analytical redundancy relations are capable of fault detection and especially fault isolation with only topside sensors available. Two cases are studied: drillstring washout, and a negative bias drift in the choke pressure sensor p_c.

8.1. Drillstring washout without downhole measurements

Without downhole sensors, it is difficult to distinguish between a negative drift in p_p, a positive drift in p_c, and drillstring washout (f_{wo}), as shown in Tab. 5. However, detecting that something has happened, and narrowing down the possibility to these three different scenarios, is still of great value for the drilling crew.

Topside pressure and flow measurements are plotted in Fig. 13, where the washout case consists of the first 19 minutes. In Fig. 14, the actual washout is measured as pressure drop over a valve, where there is no washout if the pressure drop is zero. The corresponding effects on the residuals are shown in Fig. 15, showing an increase in $\tilde{r}_2$ and $\tilde{r}_3$ during the washout. Also here, a

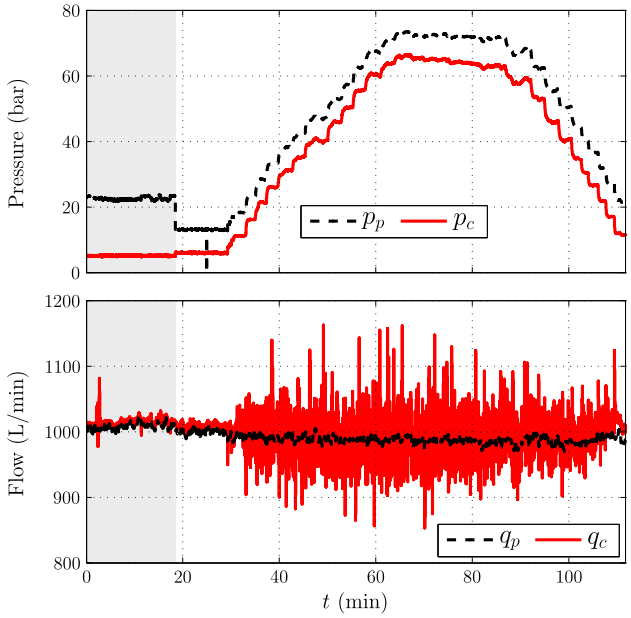

Figure 13: Pressure measurements (top) and flow measurements (bottom) of drillstring washout (grey background) and a negative bias drift in sensor p_c without downhole measurements.

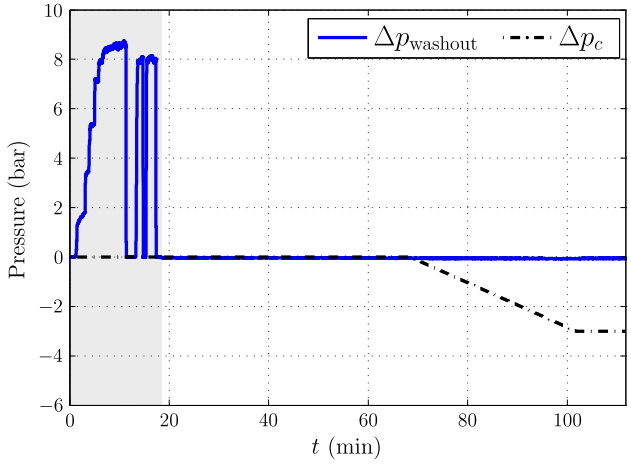

Figure 14: Drillstring washout (grey background), and artificially added negative bias drift in p_c starting at 69 minutes. None of this information is available to the diagnosis method.

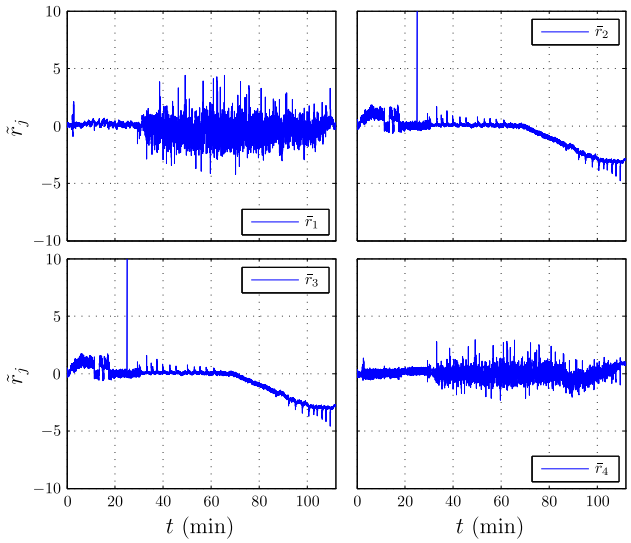

Figure 15: Residuals $\tilde{r}_1$ - $\tilde{r}_4$ for drillstring washout and negative bias drift in p_c, without downhole measurements.

statistical change detection algorithm is necessary to get sufficient detection with a low false alarm rate. The GLRT statistic is plotted in Fig. 16, showing detection of the incident, with isolation narrowed down to either positive bias in p_c, negative bias in p_p or a drillstring washout, which is the actual case.

8.2. Negative bias drift in choke pressure sensor without downhole measurements

Detection and isolation of a negative bias drift in the choke pressure sensor p_c is shown in Fig. 17, where no downhole measurements are available. The drift is ramped up from 0 to 3 bar quite slowly. For bias drift under around 1 bar (before 60 minutes), the value of $g(k)$ is below the threshold value, while for increasing drifting values the bias is isolated to the correct subgroup of incidents.

9. Discussion

Two different diagnosis scenarios using flow-loop data were tested, assuming in the first scenario that downhole pressure sensors were available, while in the second only topside sensors were used. Using downhole pressure sensors, all incidents are detectable and isolable using analytical redundancy

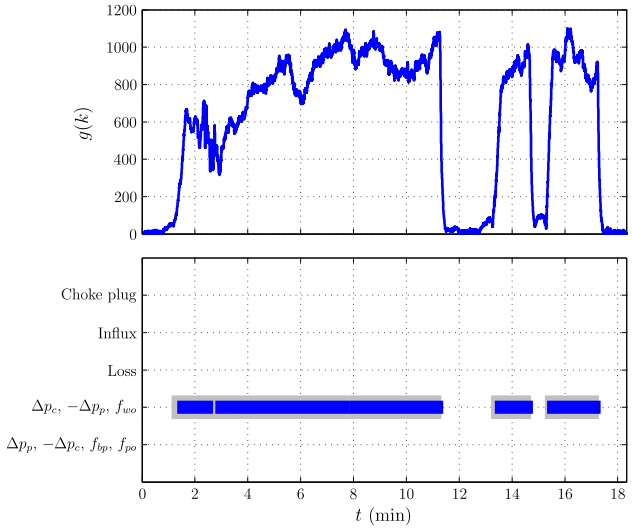

Figure 16: Detection and isolation of a washout without downhole measurements. The incident is isolated to be either a positive bias drift in p_c, a negative drift in p_p, or a drillstring washout.

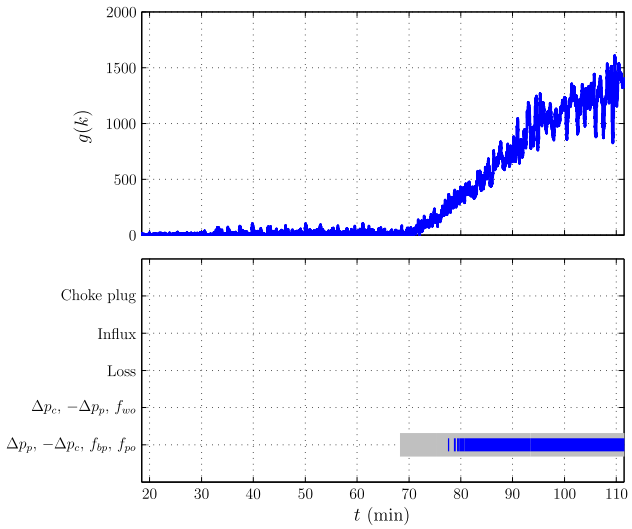

Figure 17: Detection and isolation of a negative bias drift in pressure sensor p_c without downhole measurements. The sensor fault is isolated as either a positive bias drift in p_p, a bit nozzle plugging, a pack-off, or the actual negative bias drift in p_c.

relations, except separating a pack-off from a negative drift in the measured choke pressure. Detection and isolation was successfully achieved at an early stage, with temporal false alarms only for the gas influx incident.

When using only topside measurements, the number of residuals were reduced from six to four, with the effect of greatly reducing isolation capabilities. As can be seen in Tab. 5, there are several overlaps between the different cases, especially if both negative and positive bias drift of the pressure sensors are considered. However, there is still important information in the existing isolation. A possibility to separate a drillstring washout from either a bit nozzle plugging or a pack-off is of great value for the drilling personnel.

The model used to generate the residuals is limited to hydraulic relationships between pressures and flow rates. In a real drilling rig system, there is also information about drillstring torque and the weight of the drillstring and bottomhole assembly, called weight on bit, as well as the rate of penetration. This information can be included as constraints in (3), giving increased detection and isolation capabilities. An influx can be a result of drilling into a gas pocket, called a *drilling break*, increasing the rate of penetration drastically. A pack-off will not only increase fluid friction, but also increase the rotational friction of the drillstring. This would be seen as an increase in the torque measured topside. The diagnosis framework described in this paper could easily be extended with these features, illustrating its flexibility for extending the detection and isolation capabilities.

Diagnosis of downhole incidents is also possible using adaptive observers, which was done in [7, 8]. Tab. 1 made a comparison between the methods, where one method was favorable for some properties, while the other method was best suited for others. Adaptive observers make it possible to estimate the fault magnitude, at least in some cases. This is not directly possible using analytical redundancy relations. ARR, however, make it possible to distinguish between sensor faults and actuator faults from physical incidents, a property not directly possible using adaptive observers. A complete diagnosis system may thus implement both methods, possibly combining them for improved diagnosis.

10. Conclusion

Analytical redundancy relations were used to generate residuals based on a simple hydraulics drilling model. Despite significant measurement noise,

statistical change detection of the residuals was achieved with early detection and low false alarm rates using a multivariate generalized likelihood ratio test. Data from a medium-scale horizontal flow-loop rig of 1400 meters was used to test incident diagnosis capabilities. Successful detection and isolation was achieved with the specified low false alarm rates for all of the incidents: drillstring washout; fluid loss; gas influx; bit nozzle plugging; choke plugging; as well as bias drift of the pressure sensors. The method was first tested using downhole pressure sensors, showing successful isolation of all of the different incidents. Then, using only cheaper and readily available topside measurements, the different incidents were shown to be successfully detected and isolated into subgroups of possible incidents.

Acknowledgment

Financial support from Statoil ASA and the Norwegian Research Council (NFR project 210432/E30 Intelligent Drilling) is gratefully acknowledged. Experimental data are results from ongoing internal research in the Intelligent Drilling Department in Statoil RDI. The authors also acknowledge the very valuable efforts and help from Alexey Pavlov, Henrik Manum, Glenn-Ole Kaasa, Jon Myklebost and Qin Li in planning and conducting the experiments.

[1] J. Gravdal, M. Nikolaou, Ø. Breyholtz, L. Carlsen, Improved Kick Management During MPD by Real-Time Pore-Pressure Estimation, SPE Drilling and Completion 25 (4) (2010) 577–584.

[2] E. Hauge, O. M. Aamo, J.-M. Godhavn, G. Nygaard, A novel model-based scheme for kick and loss mitigation during drilling, J. Process Control 23 (4) (2013) 463–472.

[3] E. Cayeux, E. W. Dvergsnes, G. Sælevik, Early Symptom Detection on the Basis of Real-Time Evaluation of Downhole Conditions: Principles and Results From Several North Sea Drilling Operations, SPE Drilling and Completion 27 (4) (2012) 546–558.

[4] P. Skalle, A. Aamodt, O. E. Gundersen, Detection of Symptoms for Revealing Causes Leading to Drilling Failures, SPE Drilling and Completion 28 (2) (2013) 182–193.

[5] N. Bedjaoui, E. Weyer, Algorithms for leak detection, estimation, isolation and localization in open water channels, Control Engineering Practice 19 (6) (2011) 564–573.

[6] Y. Zhang, J. Jiang, Bibliographical review on reconfigurable fault-tolerant control systems, Annual Reviews in Control 32 (2) (2008) 229–252.

[7] A. Willersrud, M. Blanke, L. Imsland, A. Pavlov, Drillstring Washout Diagnosis using Friction Estimation and Statistical Change Detection, IEEE Trans. Control Syst. Technol. (conditionally accepted).

[8] A. Willersrud, M. Blanke, L. Imsland, A. Pavlov, Fault diagnosis of downhole drilling incidents using adaptive observers and statistical change detection, J. Process Control (conditionally accepted).

[9] E. Chow, A. Willsky, Analytical redundancy and the design of robust failure detection systems, IEEE Transactions on Automatic Control 29 (7) (1984) 603–614.

[10] M. Staroswiecki, G. Comtet-Varga, Analytical redundancy relations for fault detection and isolation in algebraic dynamic systems, Automatica 37 (5) (2001) 687–699.

[11] M. Blanke, M. Kinnaert, J. Lunze, M. Staroswiecki, Diagnosis and fault-tolerant control, 2nd Edition, Springer, Berlin, 2006.

[12] L. Van Eykeren, Q. Chu, Sensor fault detection and isolation for aircraft control systems by kinematic relations, Control Engineering Practice 31 (2014) (2014) 200–210.

[13] H. M. Odendaal, T. Jones, Actuator fault detection and isolation: An optimised parity space approach, Control Engineering Practice 26 (2014) 222–232.

[14] T. Knüppel, M. Blanke, J. Østergaard, Fault diagnosis for electrical distribution systems using structural analysis, International Journal of Robust and Nonlinear Control 24 (8-9) (2014) 1446–1465.

[15] M. Basseville, Detecting Changes in Signals and Systems - A Survey, Automatica 24 (3) (1988) 309–326.

[16] J. Gertler, K. Yin, Statistical decision making for dynamic parity relations, in: Proc. IFAC World Congress, no. N, San Fransisco, CA, 1996, pp. 13–18.

[17] Y. Peng, A. Youssouf, P. Arte, M. Kinnaert, A complete procedure for residual generation and evaluation with application to a heat exchanger, IEEE Transactions on Control Systems Technology 5 (6) (1997) 542–555.

[18] T. Heyns, S. Godsill, J. de Villiers, P. Heyns, Statistical gear health analysis which is robust to fluctuating loads and operating speeds, Mechanical Systems and Signal Processing 27 (2012) (2012) 651–666.

[19] J. Gertler, R. Monajemy, Generating directional residuals with dynamic parity relations, Automatica 31 (4) (1995) 627–635.

[20] K. Yin, Minimax methods for fault isolation in the directional residual approach, Chemical Engineering Science 53 (16) (1998) 2921–2931.

[21] V. Venkatasubramanian, R. Rengaswamy, K. Yin, S. N. Kavuri, A review of process fault detection and diagnosis Part I: Quantitative model-based methods, Computers & Chemical Engineering 27 (3) (2003) 293–311.

[22] M. J. Jellison, G. Prideco, D. R. Hall, D. C. Howard, H. Tracy, R. C. Long, D. O. E. National, E. Technology, R. B. Chandler, D. S. Pixton, Telemetry Drill Pipe: Enabling Technology for the Downhole Internet, in: SPE/IADC Drilling Conference, Amsterdam, The Netherlands, 2003, pp. 1–10.

[23] D. S. Pixton, N. O. V. Intelliserv, R. A. Shishavan, H. D. Perez, J. D. Hedengren, A. Craig, Addressing UBO and MPD Challenges with Wired Drill Pipe Telemetry, in: SPE/IADC Drilling Conference and Exhibition, SPE 168953, Madrid, Spain, 2014.

[24] C. Svärd, M. Nyberg, E. Frisk, M. Krysander, Data-driven and adaptive statistical residual evaluation for fault detection with an automotive application, Mechanical Systems and Signal Processing 45 (1) (2014) 170–192.

[25] R. Isermann, P. Ballé, Trends in the application of model-based fault detection and diagnosis of technical processes, Control Engineering Practice 5 (5) (1997) 709–719.

[26] R. Patton, J. Chen, Observer-based fault detection and isolation: Robustness and applications, Control Engineering Practice 5 (5) (1997) 671–682.

[27] J. Gertler, Fault detection and isolation using parity relations, Control Engineering Practice 5 (5) (1997) 653–661.

[28] R. Isermann, Fault-Diagnosis Systems, Springer, Berlin, 2006.

[29] G.-O. Kaasa, Ø. N. Stamnes, O. M. Aamo, L. Imsland, Simplified Hydraulics Model Used for Intelligent Estimation of Downhole Pressure for a Managed-Pressure-Drilling Control System, SPE Drilling and Completion 27 (1) (2012) 127–138.

[30] L. Trave-Massuyes, T. Escobet, X. Olive, Diagnosability Analysis Based on Component-Supported Analytical Redundancy Relations, IEEE Transactions on Systems, Man, and Cybernetics - Part A: Systems and Humans 36 (6) (2006) 1146–1160.

[31] C. Sundström, E. Frisk, L. Nielsen, Selecting and Utilizing Sequential Residual Generators in FDI Applied to Hybrid Vehicles, IEEE Transactions on Systems, Man, and Cybernetics: Systems 44 (2) (2014) 172–185.

[32] M. Krysander, J. Aslund, M. Nyberg, An Efficient Algorithm for Finding Minimal Overconstrained Subsystems for Model-Based Diagnosis, IEEE Transactions on Systems, Man, and Cybernetics - Part A: Systems and Humans 38 (1) (2008) 197–206.

[33] J. Armengol, A. Bregon, T. Escobet, E. Gelso, M. Krysander, M. Nyberg, X. Olive, B. Pulido, L. Trave-Massyues, Minimal Structurally Overdetermined sets for residual generation: A comparison of alternative approaches, in: Proc. IFAC Safeprocess, Barcelona, Spain, 2009.

[34] M. Blanke, T. Lorentzen, SaTool - A software tool for structural analysis of complex automation systems, in: Proc. IFAC Safeprocess, 2006, pp. 629–634.

[35] C. Svard, M. Nyberg, E. Frisk, Realizability Constrained Selection of Residual Generators for Fault Diagnosis With an Automotive Engine Application, IEEE Transactions on Systems, Man, and Cybernetics: Systems 43 (6) (2013) 1354–1369.

[36] S. Hansen, M. Blanke, In-Flight Fault Diagnosis for Autonomous Aircraft Via Low-Rate Telemetry Channel, in: Proc. IFAC Safeprocess, Mexico City, Mexico, 2012, pp. 576–581.

[37] S. Hansen, M. Blanke, Diagnosis of Airspeed Measurement Faults for Unmanned Aerial Vehicles, IEEE Trans. Aerosp. Electron. Syst. 50 (1).

[38] S. Kotz, S. Nadarajah, Multivariate t-distribution and their applications, Cambridge University Press, Cambridge, United Kingdom, 2004.

[39] R. Galeazzi, M. Blanke, N. K. Poulsen, Early Detection of Parametric Roll Resonance on Container Ships, IEEE Trans. Control Syst. Technol. 21 (2) (2013) 489–503.

[40] M. Blanke, S. Fang, R. Galeazzi, B. J. Leira, Statistical Change Detection for Diagnosis of Buoyancy Element Defects on Moored Floating Vessels, in: IFAC Safeprocess, 2012, pp. 462–467.

[41] S. Fang, M. Blanke, B. J. Leira, Mooring System Diagnosis and Structural Reliability Control for Position Moored Vessels, Control Engineering Practice (conditionally accepted)doi:10.1016/j.conengprac.2014.11.009.

[42] A. Willersrud, L. Imsland, Fault Diagnosis in Managed Pressure Drilling Using Nonlinear Adaptive Observers, in: Proc. European Control Conference, Zürich, Switzerland, 2013, pp. 1946–1951.